

Quantum light transport in a nanophotonic waveguide coupled to an atomic ensemble

Guo-Zhu Song,^{1,*} Jin-Liang Guo,¹ Wei Nie,² Leong-Chuan Kwek,^{3,4,5,6} and Gui-Lu Long^{7,8,9,10}

¹*College of Physics and Materials Science, Tianjin Normal University, Tianjin 300387, China*

²*Theoretical Quantum Physics Laboratory, RIKEN Cluster for Pioneering Research, Wako-shi, Saitama 351-0198, Japan*

³*Centre for Quantum Technologies, National University of Singapore, 3 Science Drive 2, Singapore 117543*

⁴*Institute of Advanced Studies, Nanyang Technological University, Singapore 639673*

⁵*National Institute of Education, Nanyang Technological University, Singapore 637616*

⁶*MajuLab, CNRS-UNS-NUS-NTU International Joint Research Unit, UMI 3654, Singapore*

⁷*State Key Laboratory of Low-Dimensional Quantum Physics and*

Department of Physics, Tsinghua University, Beijing 100084, China

⁸*Beijing National Research Center for Information Science and Technology, Beijing 100084, China*

⁹*Frontier Science Center for Quantum Information, Beijing 100084, China*

¹⁰*Beijing Academy of Quantum Information Sciences, Beijing 100193, China*

(Dated: March 17, 2020)

Realizing efficient interactions between photons and multiple quantum emitters is an important ingredient in quantum optics and quantum information processing. Here we theoretically study the optical properties of an ensemble of two-level atoms coupled to a one-dimensional waveguide. In our model, the atoms are randomly located in the lattice sites along the one-dimensional waveguide. The results reveal that the optical transport properties of the atomic ensemble are influenced by the lattice constant and the filling factor of the lattice sites. We also focus on the atomic mirror configuration and quantify the effect of the inhomogeneous broadening in atomic resonant transition on the scattering spectrum. Since atoms are randomly placed in the lattice sites, we analyze the influence of the atomic spatial distributions on the transmission spectrum. Furthermore, we find that initial bunching and quantum beats appear in photon-photon correlation function of the transmitted field, which are significantly changed by filling factor of the lattice sites. With great progress to interface quantum emitters with nanophotonics, our results should be experimentally realizable in the near future.

PACS numbers: 03.67.Lx, 03.67.Pp, 42.50.Ex, 42.50.Pq

I. INTRODUCTION

In the past decades, waveguide quantum electrodynamics (QED) has raised great interest owing to its promising applications in quantum devices and quantum information technologies [1–17]. Waveguide QED describes interaction phenomena between electromagnetic fields confined to a one-dimensional (1D) waveguide and nearby quantum emitters. In practice, the waveguide can be realized with a number of physical systems such as surface plasmon nanowire [18–21], diamond waveguide [22–25], optical nanofiber [26–45], photonic crystal [46–62], and superconducting microwave transmission line [63–74]. Recently, photon transport in a 1D waveguide coupled to quantum emitters has been widely studied both in theory [1–3, 39–43, 59, 60, 66–69] and experiment [19, 23, 26, 27, 33–36, 51, 54, 64, 65].

With the real space description of the Hamiltonian and the Bethe-ansatz approach, Shen and Fan studied the transport properties of single photon scattered by a single emitter coupled to a 1D waveguide [1, 66]. They found that, a photon with frequency resonant to the two-level emitter can be completely reflected, which arises from destructive quantum interference. Then, some other meth-

ods were used to study the photon transport in a 1D waveguide, such as the input-output theory [3], the time-dependent theory [75] and Lippmann-Schwinger scattering approach [76]. Besides the single-emitter case, single-photon scattering by multiple emitters has also been studied, which gives rise to much richer optical behaviors due to multiple scattering effects. Kien *et al.* calculated the spontaneous emission from a pair of two-level atoms near a nanofiber, where a substantial radiative exchange between distant atoms was demonstrated [77]. Later, Tsoi and Law studied the interaction between a single photon and a chain of N equally spaced two-level atoms in a 1D waveguide [78]. In contrast to the single-atom case, they found that a photon can be perfectly transmitted near the resonance atomic frequency, and the positions of transmission peaks and their widths are sensitive to the relative position between atoms. Moreover, Chang *et al.* showed that an ensemble of periodically arranged two-level atoms with a specific lattice constant can form an effective cavity within the nanofiber [79].

Motivated by these important works, we here focus on the optical properties of an ensemble of two-level atoms coupled to a 1D waveguide. Due to atomic collisions during the loading process, each lattice trap site surrounding a 1D waveguide contains at most a single atom in current experiments [31, 36]. Thus, we assume that the atoms in our system are randomly trapped in the lattice along the 1D waveguide, which is different from the above cases

*Corresponding author: songguozhu@tjnu.edu.cn

where the atoms are arranged periodically. In this paper, we calculate the scattering properties of a weak coherent input field through an atomic chain and average over a large sample of atomic distributions.

In the present work, provided that the input field is monochromatic, we first study the scattering properties of a two-level atomic chain coupled to a 1D nanophotonic waveguide. The results show that the transport properties are influenced by the lattice constant and the filling factor of the lattice sites. We calculate the optical depth as a function of the lattice constant, concluding that different choices of the lattice constant do not qualitatively change the optical depth, excluding those close to $m\pi/k_a$ (m is an integer and k_a is the associated wave vector). We then focus on the atomic mirror configuration and give the reflection spectra of the incident field with different choices of the filling factors of the lattice sites. Besides, we analyze the effect of the inhomogeneous broadening in atomic resonant transition on the scattering spectrum of the input field. Moreover, since atoms are randomly located in the lattice sites, we analyze the influence of the atomic spatial distributions on the transmission of the input field. We find that the influence of atomic spatial distributions on the transmission varies with the frequency detuning. Finally, we calculate the second-order correlation function of the transmitted field with different choices of the filling factors of the lattice sites. We find that quantum beats (oscillations) [80] appear in photon-photon correlation function of the transmitted field. Moreover, when we increase the filling factor of the lattice sites, quantum beat lasts longer. Therefore, the filling factor of the lattice sites provides an efficient way to modify the quantum beats in the second-order correlation function of the transmitted field.

We have organized this article as follows: In Sec. II, we introduce the physics for an atomic chain coupled to a 1D waveguide, and present the derivation of an effective Hamiltonian for the system. In Sec. III, we study the scattering properties of a weak coherent input field through the atomic chain. Moreover, we analyze the transmission variance caused by atomic positions and compute the photon-photon correlation function of the transmitted field in the resonant case. Finally, we discuss the feasibility of our model with current experimental technology, and summarize the results in Sec. IV.

II. MODEL SYSTEM

In this section, we consider a system comprising an ensemble of two-level atoms spaced along a 1D waveguide, as shown in Fig. 1. Each atom has two electronic levels, i.e., the ground state $|g\rangle$ and the excited state $|e\rangle$. We assume that the transition with the resonance frequency ω_a between states $|g\rangle$ and $|e\rangle$ is coupled to the guided modes of the 1D dielectric waveguide. By generating an optical lattice external to the waveguide, the atoms can be trapped in fixed positions [27, 82]. Here, the frequency

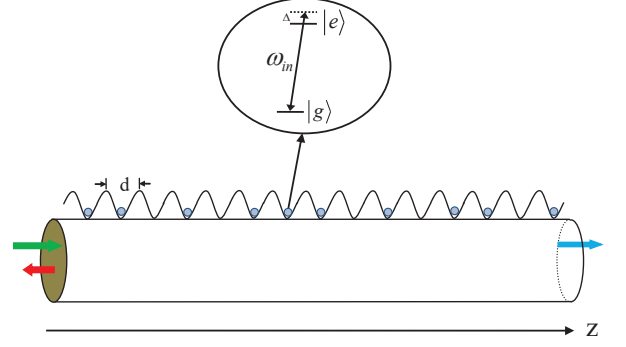


FIG. 1: (a) Schematic diagram of the propagation of an input field through a two-level atomic ensemble (grey dots) coupled to a 1D waveguide (the cylinder). The wavy line denotes the optical lattice external to the waveguide, and the lattice constant is marked by d . A weak coherent field (green arrow) is incident from left to scatter with the atomic ensemble, which produces output fields including a transmitted part (blue arrow) and a reflected part (red arrow). In practice, due to the collisional blockade mechanism [81], either zero or one atom is trapped in each lattice site [35, 36].

ω_a is assumed to be away from the waveguide cut-off frequency so that the left- and right-propagating fields can be treated as completely separate quantum fields [1, 18]. Under rotating wave approximation, the Hamiltonian of the system in real space is given by ($\hbar = 1$) [1]

$$H = \sum_{j=1}^n \omega_a \sigma_{ee}^j + i v_g \int dz \left[a_L^\dagger(z) \frac{\partial a_L(z)}{\partial z} - a_R^\dagger(z) \frac{\partial a_R(z)}{\partial z} \right] - \tilde{g} \int dz \sum_{j=1}^n \delta(z - z_j) \{ \sigma_{eg}^j [a_R(z) + a_L(z)] + \text{H.c.} \}, \quad (1)$$

where v_g is the group velocity of the field, z_j represents the position of the atom j , and a_L (a_R) denotes the annihilation operator of left (right) propagating field. The coupling constant $\tilde{g} = \sqrt{2\pi}g$ is assumed to be identical for all modes, where g denotes the single-atom coupling strength to waveguide modes. The atomic operators $\sigma_{\alpha\beta}^j = |\alpha_j\rangle\langle\beta_j|$, where $\alpha, \beta = g, e$ are energy eigenstates of the j th atom. n is the number of the atoms trapped along the waveguide.

The Heisenberg equation of the motion for the atomic operator is

$$\dot{\sigma}_{ge}^j = -i\omega_a \sigma_{ge}^j + i\tilde{g}(\sigma_{gg}^j - \sigma_{ee}^j)[a_R(z_j) + a_L(z_j)]. \quad (2)$$

Likewise, we can also obtain the Heisenberg equations of motions for left and right propagating fields in the

waveguide

$$\begin{aligned} \left(\frac{1}{v_g} \frac{\partial}{\partial t} - \frac{\partial}{\partial z}\right) a_L(z) &= \frac{i\tilde{g}}{v_g} \sum_{j=1}^n \delta(z - z_j) \sigma_{ge}^j, \\ \left(\frac{1}{v_g} \frac{\partial}{\partial t} + \frac{\partial}{\partial z}\right) a_R(z) &= \frac{i\tilde{g}}{v_g} \sum_{j=1}^n \delta(z - z_j) \sigma_{ge}^j. \end{aligned} \quad (3)$$

Then, we transform them to a co-moving frame with coordinates $z' = z$, $t' = t - z/v_g$, and get the equation of motion for a_R

$$\frac{\partial}{\partial z'} a_R(z') = \frac{i\tilde{g}}{v_g} \sum_{j=1}^n \delta(z' - z_j) \sigma_{ge}^j(t'). \quad (4)$$

Integrating over $z' \in [z - v_g t, z]$, we obtain

$$a_R(z, t) - a_R(z - v_g t) = \frac{i\tilde{g}}{v_g} \sum_{j=1}^n \int dz' \delta(z' - z_j) \sigma_{ge}^j(t'). \quad (5)$$

Since the contribution from a time earlier than $z - v_g t$ is zero, the lower limit of the integral on the right hand side of Eq. (5) can be extended to $-\infty$. We then get

$$a_R(z, t) = a_{R,in}(z - v_g t) + \frac{i\tilde{g}}{v_g} \sum_{j=1}^n \theta(z - z_j) \sigma_{ge}^j(t - \frac{z - z_j}{v_g}). \quad (6)$$

Here θ represents the Heaviside step function, and $a_{R,in}(z - v_g t)$ denotes the input field which evolves from the initial time to the present without interacting with the atoms. Similarly, the operator $a_L(z, t)$ for the left-moving field is written as

$$a_L(z, t) = a_{L,in}(z + v_g t) + \frac{i\tilde{g}}{v_g} \sum_{j=1}^n \theta(z_j - z) \sigma_{ge}^j(t - \frac{z_j - z}{v_g}). \quad (7)$$

Then, we insert Eq. (6) and Eq. (7) into Eq. (2) and get the evolution of the atomic coherence

$$\dot{\sigma}_{ge}^j = -i\omega_a \sigma_{ge}^j - \frac{\tilde{g}^2}{v_g} (\sigma_{gg}^j - \sigma_{ee}^j) \sum_l \sigma_{ge}^l(t - \frac{|z_j - z_l|}{v_g}). \quad (8)$$

By defining new operators S_{ge}^j via $\sigma_{ge}^j = S_{ge}^j e^{-i\omega_{in} t}$, we transform Eq. (8) into a slow-varying frame. Here ω_{in} denotes the frequency of an external driving field, which is close to the atomic resonance frequency ω_a with wave vector k_a . Thus, we find the equation of motion

$$\begin{aligned} \dot{S}_{ge}^j(t) &= i\Delta S_{ge}^j(t) - \frac{\Gamma_0}{2} [S_{gg}^j(t) - S_{ee}^j(t)] \\ &\quad \times \sum_l S_{ge}^l(t - \frac{|z_j - z_l|}{v_g}) e^{ik_{in}|z_j - z_l|}, \end{aligned} \quad (9)$$

where $\Delta = \omega_{in} - \omega_a$, and $k_{in} = \omega_{in}/v_g$. $\Gamma_0 = 4\pi g^2/v_g$ denotes the single-atom spontaneous emission rate into

waveguide modes. In fact, the operator on the right hand side of Eq. (9) can be expanded as

$$\begin{aligned} S_{ge}^l(t - \frac{|z_j - z_l|}{v_g}) &= S_{ge}^l(t) - \frac{|z_j - z_l|}{v_g} \dot{S}_{ge}^l(t) + \frac{1}{2} \left(\frac{|z_j - z_l|}{v_g}\right)^2 \\ &\quad \times \ddot{S}_{ge}^l(t) + \dots \end{aligned} \quad (10)$$

For small separations, i.e., $|z_j - z_l| \ll v_g$, the system is Markovian [80, 83]. In this case, the causal propagation time of the field between two atoms j and l can be neglected. Omitting higher order terms of Eq. (10), we get

$$\begin{aligned} \dot{S}_{ge}^j(t) &= -\frac{\Gamma_0}{2} [S_{gg}^j(t) - S_{ee}^j(t)] \sum_l S_{ge}^l(t) e^{ik_{in}|z_j - z_l|} \\ &\quad + i\Delta S_{ge}^j(t). \end{aligned} \quad (11)$$

From the above equation, we can extract an effective Hamiltonian for our system

$$H_{eff} = -\Delta \sum_{j=1}^n S_{ee}^j - i\frac{\Gamma_0}{2} \sum_{j,k=1}^n e^{ik_a|z_j - z_k|} S_{eg}^j S_{ge}^k. \quad (12)$$

Considering the spontaneous emission of the excited state into free space, we can add an imaginary part $-i\frac{\Gamma'_e}{2}$ to the energy of the excited state [84]. Thus, the atomic chain mediated by the 1D waveguide can be described by a non-Hermitian effective Hamiltonian [79, 83]

$$H_1 = -\sum_{j=1}^n (\Delta + i\Gamma'_e/2) S_{ee}^j - i\frac{\Gamma_0}{2} \sum_{j,k=1}^n e^{ik_a|z_j - z_k|} S_{eg}^j S_{ge}^k, \quad (13)$$

where Γ'_e denotes the decay rate of the state $|e\rangle$ into free space.

In this work, we mainly study the scattering properties of a weak coherent input field. Then, the driving part is given by $H_d = \sqrt{\frac{\Gamma_0 v_g}{2}} \mathcal{E} \sum_{j=1}^n (S_{eg}^j e^{ik_{in} z_j} + \text{H.c.})$, with \mathcal{E} being the amplitude of the weak input field (Rabi frequency $\sqrt{\frac{\Gamma_0 v_g}{2}} \mathcal{E}$). Finally, the dynamics of the atomic ensemble is described by the Hamiltonian $H = H_1 + H_d$. Since the incident field is assumed to be sufficiently weak ($\sqrt{\frac{\Gamma_0 v_g}{2}} \mathcal{E} \ll \Gamma'_e$), we can neglect quantum jumps [59]. Initially, all atoms are prepared in the ground state $|g\rangle$, and the weak coherent field is input from the left. Using input-output method [83], we obtain the transmitted (t) and reflected (r) fields

$$\begin{aligned} a_t(z) &= \mathcal{E} e^{ik_{in} z} + i\sqrt{\frac{\Gamma_0}{2v_g}} \sum_{j=1}^n S_{ge}^j e^{ik_a(z - z_j)}, \\ a_r(z) &= i\sqrt{\frac{\Gamma_0}{2v_g}} \sum_{j=1}^n S_{ge}^j e^{-ik_a(z - z_j)}. \end{aligned} \quad (14)$$

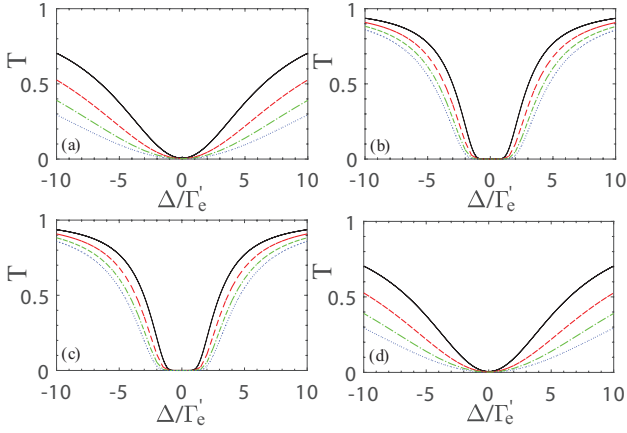


FIG. 2: The transmission spectra of the input field as a function of the frequency detuning Δ/Γ_0 for (a) $k_a d = 0$, (b) $k_a d = 1$, (c) $k_a d = \pi/2$, and (d) $k_a d = \pi$ with filling factors of the lattice sites 0.4 (black solid line), 0.6 (red dashed line), 0.8 (green dashed-dotted line), 1.0 (blue dotted line). Parameters: (a)-(d) $\mathcal{E} = 10^{-4} \sqrt{\frac{\Gamma_0}{2v_g}}$, $\Gamma_0 = 0.3\Gamma'_e$, $N = 100$.

Thus, the transmittance (T) and reflection (R) of the weak input field are given by

$$T = \frac{\langle \psi | a_t^\dagger a_t | \psi \rangle}{\mathcal{E}^2}, \quad R = \frac{\langle \psi | a_r^\dagger a_r | \psi \rangle}{\mathcal{E}^2}, \quad (15)$$

where $|\psi\rangle$ denotes the steady state of the atomic ensemble.

III. NUMERICAL RESULTS

A. Scattering properties of the input field

Here, provided that the incident field is monochromatic, we study the scattering properties of the weak input field with $N = 100$ equally spaced lattice sites along the 1D waveguide. We assume that either zero or one atom is trapped in each lattice site, and all sites are identical with a filling factor p . In other words, n atoms are placed randomly over N sites with a filling factor $p = n/N$ for each site. In Fig. 2, we show transmission spectra of the incident field as a function of the detuning Δ/Γ'_e with different values of lattice constant d . For each lattice constant, we present the transmission spectra with four different filling factors, i.e., $p = 0.4, 0.6, 0.8, 1.0$. We find that, the transmission spectrum for $k_a d = 0$ is identical to that for $k_a d = \pi$, and the transmission spectra for $k_a d = 1$ and $k_a d = \pi/2$ are the same. Moreover, after calculating many transmission spectra with different choices of lattice constant d (not shown), we conclude that different values of $k_a d$ do not qualitatively influence the transmission properties, excluding those very close to $m\pi$ (m is an integer). Besides, for any given lattice constant d , when we increase the filling factor, the lineshapes

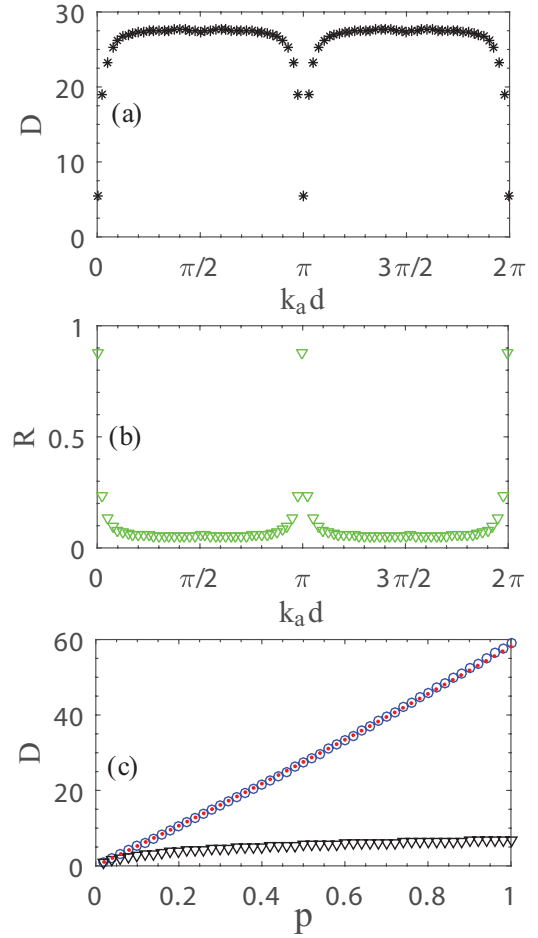


FIG. 3: (a) The optical depth D versus $k_a d$ with a filling factor $p = 0.5$. (b) The reflection of the input field as a function of $k_a d$ in the resonant case $\Delta = 0$ with a filling factor $p = 0.5$. (c) The optical depth D versus the filling factor p for $k_a d = 1$ (red dots), $k_a d = \pi/2$ (blue circles) and $k_a d = \pi$ (black down-triangles). Parameters: (a)-(c) $\mathcal{E} = 10^{-4} \sqrt{\frac{\Gamma_0}{2v_g}}$, $\Gamma_0 = 0.3\Gamma'_e$, $N = 100$.

of the transmission spectra exhibit significant broadening, as shown in Fig. 2. This is because, the collective decay rates of the atoms into the waveguide modes become enhanced when the filling factor of the lattice sites rises. Different from the Lorentzian line shape in the transmission spectrum of the single two-level atom case [1], we find that the transmission for an atomic array is approximately zero in a window centered at $\Delta = 0$ for the cases $k_a d = \pi/2$ and $k_a d = 1.0$, as shown in Figs. 2(b)-2(c).

The opacity of a medium is described by the optical depth D , where $T(\Delta = 0) = e^{-D}$. In Fig. 3(a), we calculate the optical depth as a function of $k_a d$ with a filling factor $p = 0.5$. We find that different choices of $k_a d$ do not qualitatively change the optical depth, excluding those close to $m\pi$. This is consistent with the conclusion about the influence of the lattice constant on

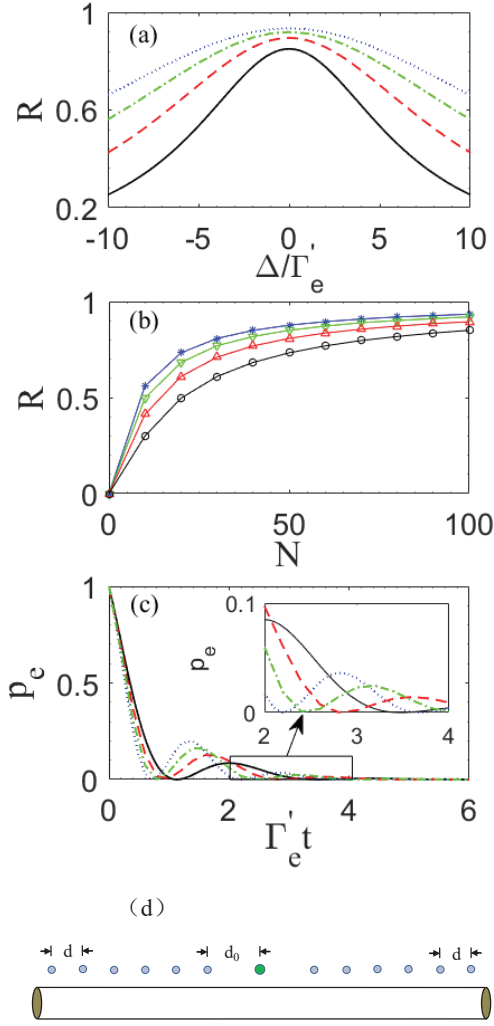


FIG. 4: (a) Reflection spectra of the input field for the filling factors 0.4 (black solid line), 0.6 (red dashed line), 0.8 (green dashed-dotted line), 1.0 (blue dotted line). (b) The reflection of the input field in the resonant case $\Delta = 0$ as a function of the number N of the lattice sites for the filling factors 0.4 (black circles), 0.6 (red up-triangles), 0.8 (green down-triangles), 1.0 (blue asterisks). (c) The population p_e of an initially excited atom (green dot in (d)) inside an atomic cavity (i.e., two sets of atomic Bragg mirrors shown in (d)) with the filling factors 0.4 (black solid line), 0.6 (red dashed line), 0.8 (green dashed-dotted line), 1.0 (blue dotted line), respectively. (d) An initially excited atom (green dot) inside an atomic cavity (two sets of grey dots) with $k_a d_0 = 1.5\pi$ and $k_a d = \pi$. (a)-(c) $\mathcal{E} = 10^{-4} \sqrt{\frac{\Gamma_0}{2v_g}}$, $\Gamma_0 = 0.3\Gamma'_e$, $k_a d = \pi$. (a) and (c) $N = 100$.

the transmission mentioned above. For $k_a d = m\pi$, the optical depth is much smaller than that for the condition $k_a d \neq m\pi$, as shown in Fig. 3(a). In fact, the case $k_a d = m\pi$, with m being an integer, corresponds to the atomic mirror configuration [79, 85]. For clear presentation, in Fig. 3(b), we present the reflection of the input field in the resonant case $\Delta = 0$ as a function of $k_a d$ with

a filling factor $p = 0.5$. We find that, the reflection of the input field in the case $k_a d = m\pi$ is much larger than those for $k_a d \neq m\pi$. Especially, for the case $k_a d = m\pi$, we find that an array of N atoms is equivalent to an effective ‘superatom’ with N times the coupling strength to the 1D waveguide (not shown). Thus it is possible to use such an atomic ensemble to compensate for the fact that the ratio Γ_0/Γ'_e is small for an individual atom and then the input field is strongly reflected. Moreover, in Fig. 3(c), we calculate the optical depth D as a function of the filling factor p for three choices of the lattice constant, i.e., $k_a d = 1, \pi/2, \pi$. The results show that, for the case $k_a d \neq m\pi$, such as $k_a d = 1$ and $k_a d = \pi/2$, the optical depth is almost not influenced by the choices of the lattice constant d . We also observe that the optical depth scales linearly with the filling factor p for the case $k_a d \neq m\pi$. While for the case $k_a d = m\pi$, such as $k_a d = \pi$, the optical depth changes slowly with the filling factor of the lattice sites.

To proceed, we focus on the atomic mirror configuration, e.g., the case $k_a d = \pi$. In Fig. 4(a), we give reflection spectra of the incident field as a function of the detuning Δ/Γ'_e with four choices of filling factor. We find that a high filling factor results in an increase in the reflection of the input field. In fact, for a resonant input field, a large number of periodically arranged atoms with a lattice constant $d = m\pi/k_a$ can be regarded as an atomic Bragg mirror [79, 85]. This effect is not sensitive to the filling imperfections and depends mainly on the choice of the lattice constant. Moreover, in the resonant case $\Delta = 0$, as shown in Fig. 4(b), the reflection of the atomic Bragg mirror is enhanced by large number N of lattice sites. In fact, for a modest filling factor, when the number of the lattice sites is sufficiently large, the reflection of the atomic Bragg mirror will approach to 100%. For example, with the filling factor being 0.6, the reflection of the atomic chain in the resonant case is 98.6% when the number of the lattice sites is 1000 [35, 36]. In particular, two sets of such atomic Bragg mirrors can form a cavity for an atom located between them, which is shown in Fig. 4(d). Here, the distance d_0 between the central atom and the nearest neighbors in the atomic mirrors satisfies the condition $k_a d_0 = 1.5\pi$, such that the central atom is located at the atomic cavity anti-node to maximize the coupling. As shown in Fig. 4(c), we calculate the population p_e of an initially excited atom inside an atomic cavity with four choices of the filling factors. The results reveal that vacuum Rabi oscillations occur between the excited central atom and the atomic cavity. Moreover, the higher the filling factor of the lattice sites is, the stronger the vacuum Rabi oscillation becomes. This is because the reflection of the atomic cavity rises when we increase the filling factor, which is shown in Fig. 4(a).

In the above discussions, we assume that these two-level atoms trapped in the lattice are the same. While, due to strong trap light fields, inhomogeneous broadening of atomic transitions exists in practical experi-

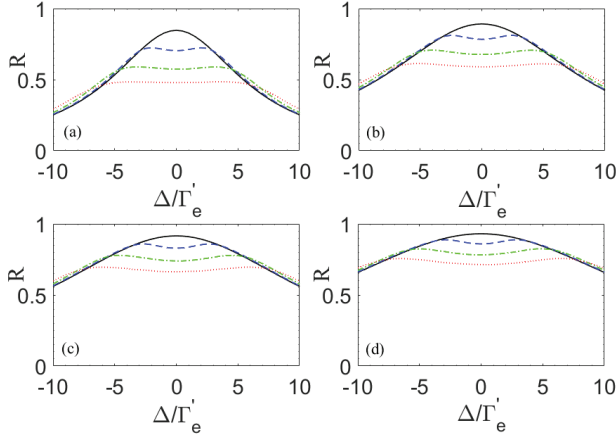


FIG. 5: Reflection spectra of the incident field as a function of the detuning Δ/Γ'_e for $\sigma_{ih} = 0$ (black solid line), $\sigma_{ih} = 1.0\Gamma'_e$ (blue dashed line), $\sigma_{ih} = 2.0\Gamma'_e$ (green dashed-dotted line), $\sigma_{ih} = 3.0\Gamma'_e$ (red dotted line) with filling factors (a) $p = 0.4$, (b) $p = 0.6$, (c) $p = 0.8$, (d) $p = 1.0$. Parameters: (a)-(d) $\mathcal{E} = 10^{-4} \sqrt{\frac{\Gamma_0}{2v_g}}$, $k_a d = \pi$, $\Gamma_0 = 0.3\Gamma'_e$, $N = 100$.

ment. Here, we consider the inhomogeneous broadening by assigning a random Gaussian distributed detuning Δ_{ih} with a standard deviation σ_{ih} to each atom. The probability density is $\rho_{ih}(\Delta_{ih}) = \frac{1}{\sigma_{ih}\sqrt{2\pi}} \exp(-\frac{\Delta_{ih}^2}{2\sigma_{ih}^2})$. As shown in Fig. 5, we show the influence of Gaussian inhomogeneous broadening of atomic transitions on the reflection of atomic Bragg mirror, e.g., the case $k_a d = \pi$. We find that, for a fixed filling factor, when the standard deviation σ_{ih} increases, the reflection in a region of the frequency detuning around $\Delta = 0$ decreases. That is, the reflection of the atomic cavity shown in Fig. 4(d) is weakened by the inhomogeneous broadening of atomic transitions. The results reveal that, for $|\Delta| \gg \Gamma'_e$, the reflection of the atomic Bragg mirror is almost robust to the exist of the inhomogeneous broadening of the atomic transition. Besides, in Fig. 6, we also calculate transmission spectra of the input field for the case $k_a d = \pi/2$ with four filling factors for $\sigma_{ih} = 0, \Gamma'_e, 2\Gamma'_e, 3\Gamma'_e$. We find that, for a fixed filling factor, when the standard deviation σ_{ih} is changed from 0 to $3.0\Gamma'_e$, lineshapes of the transmission spectra exhibit significant broadening. Moreover, for a fixed σ_{ih} , the higher the filling factor of the lattice sites is, the broader the lineshape of the transmission spectrum becomes. In particular, with $p = 0.4$, when the standard deviation σ_{ih} is sufficiently large, e.g., $\sigma_{ih} = 3.0\Gamma'_e$, a window occurs centred on $\Delta = 0$ where the transmittance is no longer approximately zero.

B. Transmission variance caused by atomic positions

In the present work, atoms are randomly located at these lattice sites along the 1D waveguide. We thus

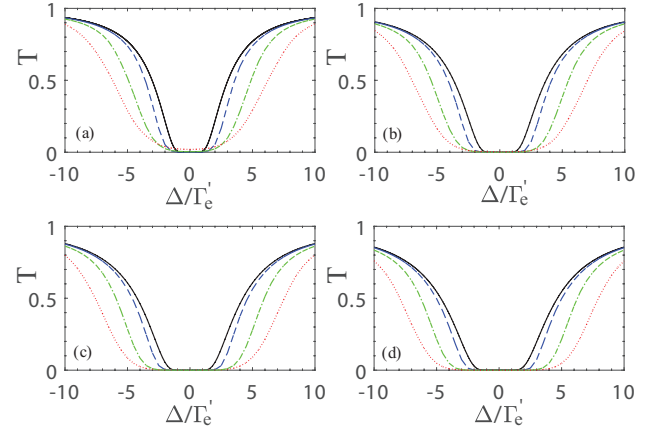


FIG. 6: Transmission spectra of the incident field as a function of the detuning Δ/Γ'_e for $\sigma_{ih} = 0$ (black solid line), $\sigma_{ih} = 1.0\Gamma'_e$ (blue dashed line), $\sigma_{ih} = 2.0\Gamma'_e$ (green dashed-dotted line), $\sigma_{ih} = 3.0\Gamma'_e$ (red dotted line) with filling factors (a) $p = 0.4$, (b) $p = 0.6$, (c) $p = 0.8$, (d) $p = 1.0$. Parameters: (a)-(d) $\mathcal{E} = 10^{-4} \sqrt{\frac{\Gamma_0}{2v_g}}$, $k_a d = \pi/2$, $\Gamma_0 = 0.3\Gamma'_e$, $N = 100$.

study the mean optical properties, averaging transmissions and reflections of the input field over many random spatial configurations. To calculate the influence of the atomic spatial distributions on the transmission of the input field, we define the variance s^2 as

$$s^2 = \frac{1}{q} \sum_{i=1}^q (T_i - \bar{T})^2. \quad (16)$$

Here, q represents the sample size of the atomic spatial configurations, T_i denotes the transmission of the input field for the i th sample, and \bar{T} is the average transmission for all samples.

In Fig. 7, we give the variance s^2 of the transmission in two cases, i.e., $k_a d = m\pi$ (e.g., $k_a d = \pi$) and $k_a d \neq m\pi$ (e.g., $k_a d = \pi/2$), where m is an integer. For each case, we average over 1000 samples of atomic spatial distributions with four filling factors, i.e., $p = 0.2, 0.4, 0.6, 0.8$. For the two cases $k_a d = m\pi$ and $k_a d \neq m\pi$, the similarities of the variance s^2 are: (i) the plot is symmetric for the frequency detuning, which is consistent with the transmission spectra shown in Fig. 2; (ii) there are two peaks around the resonance frequency $\Delta = 0$. When the detuning is at the positions of the peaks, the effect of the atomic spatial configurations on the transmission is the most obvious; (iii) for a large detuning, the variance s^2 approaches zero. In other words, the input photon transmits the atomic chain with almost no interaction for any random spatial configuration when $\Delta \gg \Gamma'_e$. Differently, in the case $k_a d \neq m\pi$, the results show that the variance s^2 is approximately zero in a region of the frequency detuning around $\Delta = 0$. This phenomenon is consistent with the transmission spectra shown in Figs. 2(b)-2(c), where the transmission of the input field is approximately zero in a window centred on $\Delta = 0$. That

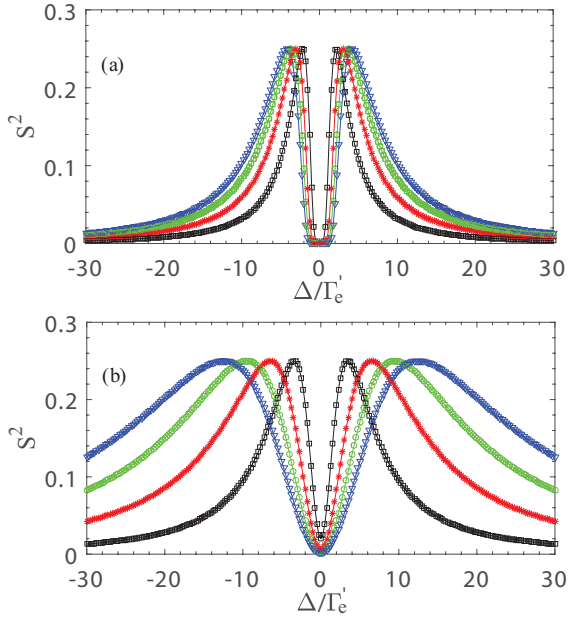


FIG. 7: The variance s^2 of the transmission T as a function of the frequency detuning Δ/Γ'_e for (a) $k_a d = \pi/2$, (b) $k_a d = \pi$ with filling factors 0.2 (black line with squares), 0.4 (red line with asterisks), 0.6 (green line with circles), 0.8 (blue line with down triangles). Here, 1000 samples of atomic positions are averaged per detuning with $\mathcal{E} = 10^{-4} \sqrt{\frac{\Gamma_0}{2v_g}}$, $\Gamma_0 = 0.3\Gamma'_e$, $N = 100$, $\sigma_{ih} = 0$.

is, for any given atomic spatial configuration in the case $k_a d \neq m\pi$, no transmission occurs in the region around $\Delta = 0$. Besides, we also observe that the positions of the two peaks in the case $k_a d = m\pi$ are more sensitive to the filling factor of the lattice sites than that in the case $k_a d \neq m\pi$.

C. Two-photon correlation

Correlation between photons is a main feature of non-classical light, which are characterized by photon-photon correlation function (second-order correlation function) $g^2(t)$ [86]. For a weak coherent state in our system, the photon-photon correlation function g^2 of the output field is defined as

$$g_\alpha^{(2)}(\tau) = \frac{\langle \psi | a_\alpha^\dagger(z) e^{iH\tau} a_\alpha^\dagger(z) a_\alpha(z) e^{-iH\tau} a_\alpha(z) | \psi \rangle}{|\langle \psi | a_\alpha^\dagger(z) a_\alpha(z) | \psi \rangle|^2}. \quad (17)$$

Here, $|\psi\rangle$ is the steady-state wave vector and $\alpha = T, R$.

Now, with a weak input field ($\sqrt{\frac{\Gamma_0 v_g}{2}} \mathcal{E} \ll \Gamma'_e$), we discuss the photon-photon correlation function of the output field in the resonant case $\Delta = 0$. In Fig. 8, we give the photon correlation function of the transmitted field with four choices of the filling factor, i.e., $p = 0.1, 0.2, 0.3, 0.4$. The results show that strong initial bunching appears in the transmitted field in each case, i.e., $g_T^{(2)}(t=0) \gg 1$.

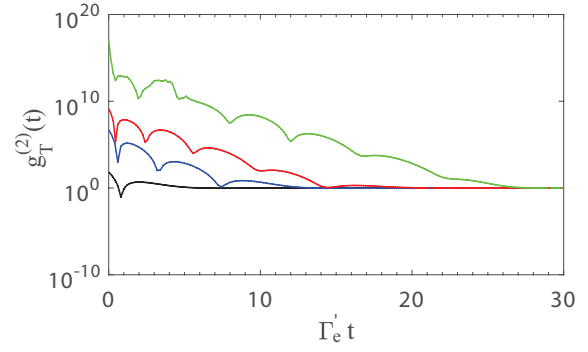


FIG. 8: The photon-photon correlation function $g_T^{(2)}(t)$ of the transmitted field in the resonant case $\Delta = 0$ for the filling factors 0.1 (black line), 0.2 (blue line), 0.3 (red line), 0.4 (green line). Parameters: $\mathcal{E} = 10^{-4} \sqrt{\frac{\Gamma_0}{2v_g}}$, $k_a d = \pi/2$, $N = 100$, $\Gamma_0 = 0.3\Gamma'_e$, $\sigma_{ih} = 0$.

When we increase the filling factor, the initial bunching becomes much stronger. Furthermore, we find quantum beats in the photon-photon correlation function of the transmitted field. Evidently, the higher the filling factor of the lattice sites is, the more visible the quantum beat becomes. By comparing these four cases shown in Fig. 8, we find that quantum beat in the photon-photon correlation function $g_T^{(2)}$ lasts longer when we increase the filling factor. The phenomena mentioned above reveal that many-body quantum systems significantly modify nonclassical property of light in the waveguide.

IV. DISCUSSION AND SUMMARY

Experimentally, our model may be realized in the current nanofiber system. In Refs. [35, 36], arrays of cesium atoms are trapped in the evanescent field of a tapered optical fiber. For a cesium atom, the ground and excited states are chosen as $|g\rangle = \{6S_{1/2}, F=4\}$ and $|e\rangle = \{6P_{3/2}, F=5\}$, respectively. The optical lattice for trapping atoms can be constructed by a pair of horizontally polarized red-detuned counterpropagating beams (wavelength $\lambda_{trap} = 1057$ nm and power $P_{trap} \approx 2 \times 1.3$ mW) and a vertically polarized blue-detuned beam (wavelength $\lambda_{blue} = 780$ nm and power $P_{blue} = 14$ mW). In their experiments, cesium atoms are first loaded from a background vapor to a 6-beam magneto-optical trap, and then they are loaded into an optical lattice via sub-Doppler cooling. Because of atomic collisions during the loading process [81], each trap site in their device hosts at most a single atom, which is consistent with the assumption in the present work. In Ref. [36], to avoid saturation, experimentalists adopt an extremely weak probe field with a power of $P_{input} = 150$ pW. Finally, with the techniques mentioned above, it is able to trap thousands of atoms in the lattice sites along the 1D waveguide as in Refs. [35, 36].

In conclusion, in this work we study scattering properties of an ensemble of two-level atoms coupled to a 1D waveguide. Since the precise control of the atomic positions is still challenging in nanophotonic waveguide system, we assume that the atoms in this work are randomly placed in the lattice along the 1D waveguide. With the effective non-Hermitian Hamiltonian, we calculate the transmission spectrum of a weak coherent input field, concluding that the optical transport properties are influenced by lattice constant and the filling factor of the lattice sites. We compute the optical depth as a function of the lattice constant, and the results reveal that the optical depth is reduced when lattice constant is close to $m\pi/k_a$. We then focus on the atomic mirror configuration and give the reflection spectra of the incident field with different filling factors of the lattice sites. We also quantify the influence of the inhomogeneous broadening in atomic resonant transition on the transmission, and find that the lineshape of the transmission spectrum exhibits significant broadening when the standard deviation σ_{ih} becomes larger. Besides, we find that the transmission variance, caused by atomic spatial distributions, for the atom mirror configuration ($k_a d = m\pi$) is distinct

from other cases. Finally, we analyze the role of filling factor played in photon-photon correlation of the transmitted field, and find that initial bunching and quantum beats are quite sensitive to the filling factor. Since great progress has been made to interface quantum emitters with nanophotonic waveguide [87], our results in this work should be realizable in the near future.

ACKNOWLEDGMENTS

This work is supported by the National Natural Science Foundation of China (NSFC) under Grant No. 11947037 and the Program for Innovative Research in University of Tianjin under Grant No. TD13-5077. L.-C.K acknowledges support from the National Research Foundation and Ministry of Education, Singapore. G.-L.L. acknowledges support from the Center of Atomic and Molecular Nanosciences, Tsinghua University, and Beijing Advanced Innovation Center for Future Chip (ICFC).

-
- [1] J. T. Shen and S. Fan, Coherent photon transport from spontaneous emission in one-dimensional waveguides, *Opt. Lett.* **30**, 2001 (2005).
 - [2] J. T. Shen and S. Fan, Strongly Correlated Two-Photon Transport in a One-Dimensional Waveguide Coupled to a Two-Level System, *Phys. Rev. Lett.* **98**, 153003 (2007).
 - [3] S. Fan, Ş. E. Kocabaş, and J. T. Shen, Input-output formalism for few-photon transport in one-dimensional nanophotonic waveguides coupled to a qubit, *Phys. Rev. A* **82**, 063821 (2010).
 - [4] L. Zhou, L. P. Yang, Y. Li, and C. P. Sun, Quantum Routing of Single Photons with a Cyclic Three-Level System, *Phys. Rev. Lett.* **111**, 103604 (2013).
 - [5] P. Lodahl, S. Mahmoodian, and S. Stobbe, Interfacing single photons and single quantum dots with photonic nanostructures, *Rev. Mod. Phys.* **87**, 347 (2015).
 - [6] Z. Liao, X. Zeng, H. Nha, and M. S. Zubairy, Photon transport in a one-dimensional nanophotonic waveguide QED system, *Phys. Scr.* **91**, 063004 (2016).
 - [7] D. Roy, C. M. Wilson, and O. Firstenberg, Strongly interacting photons in one-dimensional continuum, *Rev. Mod. Phys.* **89**, 021001 (2017).
 - [8] M. T. Manzoni, D. E. Chang, and J. S. Douglas, Simulating quantum light propagation through atomic ensembles using matrix product states, *Nat. Commun.* **8**, 1743 (2017).
 - [9] S. Das, V. E. Elfving, S. Faez, and A. S. Sørensen, Interfacing Superconducting Qubits and Single Optical Photons Using Molecules in Waveguides, *Phys. Rev. Lett.* **118**, 140501 (2017).
 - [10] K. Xia, F. Nori, and M. Xiao, Cavity-Free Optical Isolators and Circulators Using a Chiral Cross-Kerr Nonlinearity, *Phys. Rev. Lett.* **121**, 203602 (2018).
 - [11] Z. H. Chen, Y. Zhou, and J. T. Shen, Entanglement-preserving approach for reservoir-induced photonic dissipation in waveguide QED systems, *Phys. Rev. A* **98**, 053830 (2018).
 - [12] D. E. Chang, J. S. Douglas, A. González-Tudela, C.-L. Hung, and H. J. Kimble, Colloquium: Quantum matter built from nanoscopic lattices of atoms and photons, *Rev. Mod. Phys.* **90**, 031002 (2018).
 - [13] J. Zhang, X. D. Yu, G. L. Long, and Q. K. Xue, Topological dynamical decoupling, *Sci. China-Phys. Mech. Astron.* **62**, 120362 (2019).
 - [14] M. Wang, R. Wu, J. Lin, J. Zhang, Z. Fang, Z. Chai, and Y. Cheng, Chemo-mechanical polish lithography: A pathway to low loss large-scale photonic integration on lithium niobate on insulator, *Quantum Eng.* **1**, e9 (2019).
 - [15] F. Dinc, I. Ercan, and A. M. Brańczyk, Exact Markovian and non-Markovian time dynamics in waveguide QED: collective interactions, bound states in continuum, superradiance and subradiance, *Quantum* **3**, 213 (2019).
 - [16] D. E. Liu, Sensing Kondo correlations in a suspended carbon nanotube mechanical resonator with spin-orbit coupling, *Quantum Eng.* **1**, e10 (2019).
 - [17] R. Osellame, New effective technique to produce waveguides in lithium niobate on insulator (LNOI), *Quantum Eng.* **1**, e11 (2019).
 - [18] D. E. Chang, A. S. Sørensen, E. A. Demler, and M. D. Lukin, A single-photon transistor using nanoscale surface plasmons, *Nat. Phys.* **3**, 807 (2007).
 - [19] A. V. Akimov, A. Mukherjee, C. L. Yu, D. E. Chang, A. S. Zibrov, P. R. Hemmer, H. Park, and M. D. Lukin, Quantum matter built from nanoscopic lattices of atoms and photons, *Nature (London)* **450**, 402 (2007).
 - [20] A. Gonzalez-Tudela, D. Martin-Cano, E. Moreno, L. Martin-Moreno, C. Tejedor, and F. J. Garcia-Vidal, Entanglement of Two Qubits Mediated by One-Dimensional

- Plasmonic Waveguides, *Phys. Rev. Lett.* **106**, 020501 (2011).
- [21] G. M. Akselrod, C. Argyropoulos, T. B. Hoang, C. Ciraci, C. Fang, J. Huang, D. R. Smith, and M. H. Mikkelsen, Probing the mechanisms of large Purcell enhancement in plasmonic nanoantennas, *Nature Photonics* **8**, 835 (2014).
- [22] J. Claudon, J. Bleuse, N. S. Malik, M. Bazin, P. Jaffrennou, N. Gregersen, C. Sauvan, P. Lalanne, and J. M. Gérard, A highly efficient single-photon source based on a quantum dot in a photonic nanowire, *Nat. Photon.* **4**, 174 (2010).
- [23] T. M. Babinec, J. M. Hausmann, M. Khan, Y. Zhang, J. R. Maze, P. R. Hemmer, and M. Lončar, A diamond nanowire single-photon source, *Nat. Nanotechnol.* **5**, 195 (2010).
- [24] H. Clevenson, M. E. Trusheim, C. Teale, T. Schröder, D. Braje, and D. Englund, Broadband magnetometry and temperature sensing with a light-trapping diamond waveguide, *Nat. Phys.* **11**, 393 (2015).
- [25] A. Sipahigil, R. E. Evans, D. D. Sukachev, M. J. Burek, J. Borregaard, M. K. Bhaskar, C. T. Nguyen, J. L. Pacheco, H. A. Atikian, C. Meuwly, R. M. Camacho, F. Jelezko, E. Bielejec, H. Park, M. Lončar, and M. D. Lukin, An integrated diamond nanophotonics platform for quantum-optical networks, *Science* **354**, 847 (2016).
- [26] B. Dayan, A. S. Parkins, T. Aoki, E. P. Ostby, K. J. Vahala, and H. J. Kimble, A photon turnstile dynamically regulated by one atom, *Science* **319**, 1062 (2008).
- [27] E. Vetsch, D. Reitz, G. Sagué, R. Schmidt, S. T. Dawkins, and A. Rauschenbeutel, Optical Interface Created by Laser-Cooled Atoms Trapped in the Evanescent Field Surrounding an Optical Nanofiber, *Phys. Rev. Lett.* **104**, 203603 (2010).
- [28] S. T. Dawkins, R. Mitsch, D. Reitz, E. Vetsch, and A. Rauschenbeutel, Dispersive Optical Interface Based on Nanofiber-Trapped Atoms, *Phys. Rev. Lett.* **107**, 243601 (2011).
- [29] D. Reitz, C. Sayrin, R. Mitsch, P. Schneeweiss, and A. Rauschenbeutel, Coherence Properties of Nanofiber-Trapped Cesium Atoms, *Phys. Rev. Lett.* **110**, 243603 (2013).
- [30] J. Petersen, J. Volz, and A. Rauschenbeutel, Chiral nanophotonic waveguide interface based on spin-orbit interaction of light, *Science* **346**, 67 (2014).
- [31] R. Mitsch, C. Sayrin, B. Albrecht, P. Schneeweiss, and A. Rauschenbeutel, Quantum state-controlled directional spontaneous emission of photons into a nanophotonic waveguide, *Nat. Commun.* **5**, 5713 (2014).
- [32] F. Le Kien and A. Rauschenbeutel, Anisotropy in scattering of light from an atom into the guided modes of a nanofiber, *Phys. Rev. A* **90**, 023805 (2014).
- [33] C. Sayrin, C. Clausen, B. Albrecht, P. Schneeweiss, and A. Rauschenbeutel, Storage of fiber-guided light in a nanofiber-trapped ensemble of cold atoms, *Optica* **2**, 353 (2015).
- [34] B. Gouraud, D. Maxein, A. Nicolas, O. Morin, and J. Laurat, Demonstration of a Memory for Tightly Guided Light in an Optical Nanofiber, *Phys. Rev. Lett.* **114**, 180503 (2015).
- [35] N. V. Corzo, B. Gouraud, A. Chandra, A. Goban, A. S. Sheremet, D. V. Kupriyanov, and J. Laurat, Large Bragg Reflection from One-Dimensional Chains of Trapped Atoms Near a Nanoscale Waveguide, *Phys. Rev. Lett.* **117**, 133603 (2016).
- [36] H. L. Sørensen, J. B. Béguin, K. W. Kluge, I. Iakoupov, A. S. Sørensen, J. H. Müller, E. S. Polzik, and J. Appel, Coherent Backscattering of Light Off One-Dimensional Atomic Strings, *Phys. Rev. Lett.* **117**, 133604 (2016).
- [37] G. Z. Song, Q. Liu, J. Qiu, G. J. Yang, F. Alzahrani, A. Hobiny, F. G. Deng, and M. Zhang, Heralded quantum gates for atomic systems assisted by the scattering of photons off single emitters, *Ann. Phys. (NY)* **387**, 152 (2017).
- [38] P. Solano, P. B. Blostein, F. K. Fatemi, L. A. Orozco, and S. L. Rolston, Super-radiance reveals infinite-range dipole interactions through a nanofiber, *Nat. Commun.* **8**, 1857 (2017).
- [39] W. B. Yan, W. Y. Ni, J. Zhang, F. Y. Zhang, and H. Fan, Tunable single-photon diode by chiral quantum physics, *Phys. Rev. A* **98**, 043852 (2018).
- [40] D. C. Yang, M. T. Cheng, X. S. Ma, J. P. Xu, C. J. Zhu, and X. S. Huang, Phase-modulated single-photon router, *Phys. Rev. A* **98**, 063809 (2018).
- [41] G. Z. Song, E. Munro, W. Nie, F. G. Deng, G. J. Yang, and L. C. Kwek, Photon scattering by an atomic ensemble coupled to a one-dimensional nanophotonic waveguide, *Phys. Rev. A* **96**, 043872 (2017).
- [42] M. T. Cheng, J. P. Xu, and G. S. Agarwal, Waveguide transport mediated by strong coupling with atoms, *Phys. Rev. A* **95**, 053807 (2017).
- [43] C. H. Yan, Y. Li, H. D. Yuan, and L. F. Wei, Targeted photonic routers with chiral photon-atom interactions, *Phys. Rev. A* **97**, 023821 (2018).
- [44] S. Kato, N. Német, K. Senga, S. Mizukami, X. Huang, S. Parkins, and T. Aoki, Observation of dressed states of distant atoms with delocalized photons in coupled-cavities quantum electrodynamics, *Nat. Commun.* **10**, 1160 (2019).
- [45] G. Buonaiuto, R. Jones, B. Olmos, and I. Lesanovsky, Dynamical creation and detection of entangled many-body states in a chiral atom chain, *New J. Phys.* **21**, 113021 (2019).
- [46] T. Lund-Hansen, S. Stobbe, B. Julsgaard, H. Thyrrstrup, T. Sünner, M. Kamp, A. Forchel, and P. Lodahl, Experimental Realization of Highly Efficient Broadband Coupling of Single Quantum Dots to a Photonic Crystal Waveguide, *Phys. Rev. Lett.* **101**, 113903 (2008).
- [47] J. D. Thompson, T. G. Tiecke, N. P. de Leon, J. Feist, A. V. Akimov, M. Gullans, A. S. Zibrov, V. Vuletić, and M. D. Lukin, Coupling a single trapped atom to a nanoscale optical cavity, *Science* **340**, 1202 (2013).
- [48] A. Goban, C.-L. Hung, S.-P. Yu, J. D. Hood, J. A. Muniz, J. H. Lee, M. J. Martin, A. C. McClung, K. S. Choi, D. E. Chang, O. Painter, and H. J. Kimble, Atom-light interactions in photonic crystals, *Nat. Commun.* **5**, 3808 (2014).
- [49] T. G. Tiecke, J. D. Thompson, N. P. de Leon, L. R. Liu, V. Vuletić, and M. D. Lukin, Nanophotonic quantum phase switch with a single atom, *Nature (London)* **508**, 241 (2014).
- [50] M. Arcari, I. Söllner, A. Javadi, S. Lindskov Hansen, S. Mahmoodian, J. Liu, H. Thyrrstrup, E. H. Lee, J. D. Song, S. Stobbe, and P. Lodahl, Near-Unity Coupling Efficiency of a Quantum Emitter to a Photonic Crystal Waveguide, *Phys. Rev. Lett.* **113**, 093603 (2014).
- [51] S.-P. Yu, J. D. Hood, J. A. Muniz, M. J. Martin, R. Norte, C.-L. Hung, S. M. Meenehan, J. D. Co-

- hen, O. Painter, and H. J. Kimble, Nanowire photonic crystal waveguides for single-atom trapping and strong light-matter interactions, *Appl. Phys. Lett.* **104**, 111103 (2014).
- [52] A. González-Tudela, V. Paulisch, D. E. Chang, H. J. Kimble, and J. I. Cirac, Deterministic Generation of Arbitrary Photonic States Assisted by Dissipation, *Phys. Rev. Lett.* **115**, 163603 (2015).
- [53] A. B. Young, A. C. T. Thijssen, D. M. Beggs, P. Androvitsaneas, L. Kuipers, J. G. Rarity, S. Hughes, and R. Oulton, Polarization Engineering in Photonic Crystal Waveguides for Spin-Photon Entanglers, *Phys. Rev. Lett.* **115**, 153901 (2015).
- [54] A. González-Tudela, C. L. Hung, D. E. Chang, J. I. Cirac, and H. J. Kimble, Subwavelength vacuum lattices and atom-atom interactions in two-dimensional photonic crystals, *Nat. Photonics* **9**, 320 (2015).
- [55] J. S. Douglas, H. Habibian, C. L. Hung, A. V. Gorshkov, H. J. Kimble, and D. E. Chang, Quantum many-body models with cold atoms coupled to photonic crystals, *Nat. Photonics* **9**, 326 (2015).
- [56] T. Shi, Y.-H. Wu, A. González-Tudela, and J. I. Cirac, Bound States in Boson Impurity Models, *Phys. Rev. X* **6**, 021027 (2016).
- [57] J. D. Hood, A. Goban, A. Asenjo-Garcia, M. Lu, S.-P. Yu, D. E. Chang, and H. J. Kimble, Atom-atom interactions around the band edge of a photonic crystal waveguide, *Proc. Natl. Acad. Sci. U.S.A.* **113**, 10507 (2016).
- [58] J. S. Douglas, T. Caneva, and D. E. Chang, Photon Molecules in Atomic Gases Trapped Near Photonic Crystal Waveguides, *Phys. Rev. X* **6**, 031017 (2016).
- [59] E. Munro, L. C. Kwek, and D. E. Chang, Optical properties of an atomic ensemble coupled to a band edge of a photonic crystal waveguide, *New J. Phys.* **19**, 083018 (2017).
- [60] G. Z. Song, E. Munro, W. Nie, L. C. Kwek, F. G. Deng, and G. L. Long, Photon transport mediated by an atomic chain trapped along a photonic crystal waveguide, *Phys. Rev. A* **98**, 023814 (2018).
- [61] T. Li, A. Miranowicz, X. Hu, K. Xia, and F. Nori, Quantum memory and gates using a Λ -type quantum emitter coupled to a chiral waveguide, *Phys. Rev. A* **97**, 062318 (2018).
- [62] A. P. Burgersa, L. S. Penga, J. A. Muniza, A. C. McClunga, M. J. Martina, and H. J. Kimble, Clocked atom delivery to a photonic crystal waveguide, *Proc. Natl. Acad. Sci. U.S.A.* **116**, 456 (2019).
- [63] A. Wallraff, D. I. Schuster, A. Blais, L. Frunzio, R. S. Huang, J. Majer, S. Kumar, S. M. Girvin, and R. J. Schoelkopf, Strong coupling of a single photon to a superconducting qubit using circuit quantum electrodynamics, *Nature (London)* **431**, 162 (2004).
- [64] O. Astafiev, A. M. Zagoskin, A. A. Abdumalikov, Y. A. Pashkin, T. Yamamoto, K. Inomata, Y. Nakamura, and J. S. Tsai, Resonance fluorescence of a single artificial atom, *Science* **327**, 840 (2010).
- [65] A. F. van Loo, A. Fedorov, K. Lalumière, B. C. Sanders, A. Blais, and A. Wallraff, Photon-mediated interactions between distant artificial atoms, *Science* **342**, 1494 (2013).
- [66] J. T. Shen and S. Fan, Coherent Single Photon Transport in a One-Dimensional Waveguide Coupled with Superconducting Quantum Bits, *Phys. Rev. Lett.* **95**, 213001 (2005).
- [67] L. Zhou, Z. R. Gong, Y. X. Liu, C. P. Sun, and F. Nori, Controllable Scattering of a Single Photon inside a One-Dimensional Resonator Waveguide, *Phys. Rev. Lett.* **101**, 100501 (2008).
- [68] K. Lalumière, B. C. Sanders, A. F. van Loo, A. Fedorov, A. Wallraff, and A. Blais, Input-output theory for waveguide QED with an ensemble of inhomogeneous atoms, *Phys. Rev. A* **88**, 043806 (2013).
- [69] G. Z. Song, L. C. Kwek, F. G. Deng, and G. L. Long, Microwave transmission through an artificial atomic chain coupled to a superconducting photonic crystal, *Phys. Rev. A* **99**, 043830 (2019).
- [70] X. Gu, A. F. Kockum, A. Miranowicz, Y. X. Liu, and F. Nori, Microwave photonics with superconducting quantum circuits, *Phys. Rep.* **718-719**, 1 (2017).
- [71] Y. Liu and A. A. Houck, Quantum electrodynamics near a photonic bandgap, *Nat. Phys.* **13**, 48 (2017).
- [72] A. F. Kockum, G. Johansson, and F. Nori, Decoherence-Free Interaction Between Giant Atoms in Waveguide Quantum Electrodynamics, *Phys. Rev. Lett.* **120**, 140404 (2018).
- [73] M. Mirhosseini, E. Kim, V. S. Ferreira, M. Kalaei, A. Sipahigil, A. J. Keller, and O. Painter, Superconducting metamaterials for waveguide quantum electrodynamics, *Nat. Commun.* **9**, 3706 (2018).
- [74] N. M. Sundaresan, R. Lundgren, G. Zhu, A. V. Gorshkov, and A. A. Houck, Interacting Qubit-Photon Bound States with Superconducting Circuits, *Phys. Rev. X* **9**, 011021 (2019).
- [75] Y. Chen, M. Wubs, J. Mørk, and A. F. Koenderink, Coherent single-photon absorption by single emitters coupled to one-dimensional nanophotonic waveguides, *New J. Phys.* **13**, 103010 (2011).
- [76] J. F. Huang, T. Shi, C. P. Sun, and F. Nori, Controlling single-photon transport in waveguides with finite cross section, *Phys. Rev. A* **88**, 013836 (2013).
- [77] F. Le Kien, S. Dutta Gupta, K. P. Nayak, and K. Hakuta, Nanofiber-mediated radiative transfer between two distant atoms, *Phys. Rev. A* **72**, 063815 (2005).
- [78] T. S. Tsoi and C. K. Law, Quantum interference effects of a single photon interacting with an atomic chain inside a one-dimensional waveguide, *Phys. Rev. A* **78**, 063832 (2008).
- [79] D. E. Chang, L. Jiang, A. V. Gorshkov, and H. J. Kimble, Cavity QED with atomic mirrors, *New J. Phys.* **14**, 063003 (2012).
- [80] H. Zheng and H. U. Baranger, Persistent Quantum Beats and Long-Distance Entanglement from Waveguide-Mediated Interactions, *Phys. Rev. Lett.* **110**, 113601 (2013).
- [81] N. Schlosser, G. Reymond, and P. Grangier, Collisional Blockade in Microscopic Optical Dipole Traps, *Phys. Rev. Lett.* **89**, 023005 (2002).
- [82] A. Goban, C.-L. Hung, J. D. Hood, S.-P. Yu, J. A. Muniz, O. Painter, and H. J. Kimble, Superradiance for Atoms Trapped along a Photonic Crystal Waveguide, *Phys. Rev. Lett.* **115**, 063601 (2015).
- [83] T. Caneva, M. T. Manzoni, T. Shi, J. S. Douglas, J. I. Cirac, and D. E. Chang, Quantum dynamics of propagating photons with strong interactions: a generalized input-output formalism, *New J. Phys.* **17**, 113001 (2015).
- [84] H. J. Carmichael, *An Open Systems Approach to Quantum Optics* (Springer, Berlin, 1993).
- [85] M. Mirhosseini, E. Kim, X. Zhang, A. Sipahigil, P. B.

- Dieterle, A. J. Keller, A. Asenjo-Garcia, D. E. Chang, and O. Painter, Cavity quantum electrodynamics with atom-like mirrors, *Nature (London)* **569**, 692 (2019).
- [86] R. Loudon, *The Quantum Theory of Light*, 3rd ed. (Oxford University Press, New York, 2003).
- [87] K. P. Nayak, M. Sadgrove, R. Yalla, F. Le Kien, and K. Hakuta, Nanofiber quantum photonics, *J. Opt.* **20**, 073001 (2018).